



PERGAMON

Solid State Communications 124 (2002) 469–472

**solid
state
communications**

www.elsevier.com/locate/ssc

Ultra-small oscillation amplitude nc-AFM/STM imaging, force and dissipation spectroscopy of Si(100)(2 × 1)

H. Özgür Özer, Mehrdad Atabak, Ahmet Oral*

Department of Physics, Bilkent University, 06533 Bilkent, Ankara, Turkey

Received 23 July 2002; accepted 19 August 2002 by M. Cardona

Abstract

Si(100)(2 × 1) surface is imaged using a new nc-AFM (non-contact atomic force microscopy)/STM with sub-Ångstrom oscillation amplitudes using stiff hand-made tungsten levers. Simultaneous force gradient and scanning tunneling microscopy images of individual dimers and atomic scale defects are obtained. We measured force–distance and dissipation–distance curves with different tips. Some of the tips show long-range force interactions, whereas some others resolve short-range interatomic force interactions. We observed that the tips showing short-range force interaction give atomic resolution in force gradient scans. This result suggests that short-range force interactions are responsible for atomic resolution in nc-AFM. We also observed an increase in the dissipation as the tip is approached closer to the surface, followed by an unexpected decrease as we pass the inflection point in the energy–distance curve.

© 2002 Elsevier Science Ltd. All rights reserved.

PACS: 87.64:Dz

Keywords: A. Si (100) surface; E. nc-AFM/STM studies

1. Introduction

Short-ranged atomic forces play an important role in scanning tunneling microscopy (STM) [1]. Effects of these forces in STM have first been calculated by Ciraci [2] using ab initio methods. Atomic force microscopy (AFM) [3], invented by Binnig et al., utilizes these short-ranged forces to obtain surface topography of sample surfaces, down to atomic scale. However, measurement of these very small forces has been very difficult and was only possible in a very limited number of sample–tip configurations [4,5]. Atomic resolution in non-contact AFM (nc-AFM) [6] was finally achieved in 1995 using large oscillation amplitudes: ~1–10 nm for imaging and force spectroscopy. This large oscillation amplitude technique has some limitations and small oscillation amplitudes are usually more desirable for easier interpretation of data and quantitative imaging. Short-

range tip–sample interactions, of the order of a few Ångstroms, are believed to be responsible for atomic resolution imaging in nc-AFM [7,8]. We recently constructed an improved nc-AFM using ultra small oscillation amplitudes, down to 0.25 Å, for force–distance (F–d) spectroscopy and atomic resolution imaging [9]. Si(100)(2 × 1) reconstructed surface has been successfully imaged with nc-AFM by various groups, using large oscillation amplitudes [10,11]. In this work, we studied Si(100)(2 × 1) surface in UHV using small oscillation amplitudes, 0.25–2.5 Å, with an nc-AFM/STM.

2. Experiment

A high force resolution nc-AFM/STM [9] operating in UHV is used in our experiments. The microscope employs a sensitive fiber interferometer for high force resolution and sub-Ångstrom oscillation amplitudes can be used for imaging as well as force spectroscopy [7,12]. Home-made tungsten levers with typical stiffness of about 150 N/m are

* Corresponding author. Tel.: +90-312-290-1965; fax: +90-312-266-4579.

E-mail address: ahmet@fen.bilkent.edu.tr (A. Oral).

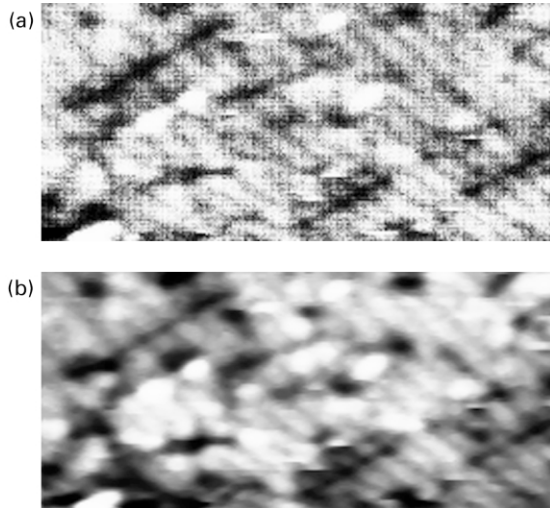


Fig. 1. Simultaneous STM (a) and force gradient (b) images of Si(100)(2 × 1). Image size is $154 \times 77 \text{ \AA}^2$, $V_{\text{tip}} = -1.5 \text{ V}$, $I_t = 1 \text{ nA}$, $A_0 = 2.4 \text{ \AA}$ and $k_0 = 157 \text{ N/m}$. Black areas correspond to more negative values in the force gradient image.

used in the experiments. The samples are cut from 525 mm thick, P-doped, Si(100) wafers oriented within 0.5° of a (001) plane. The sample is cleaned by the Shiraki method prior to introduction into UHV. Standard in situ heat treatment is employed to have an atomically clean Si(100)(2 × 1) surface. The lever is vibrated with very small oscillation amplitudes (typically sub-Ångstrom) at a frequency well below its resonance and the changes in the oscillation amplitude are recorded by using a lock-in amplifier as the sample is scanned across the tip. The microscope is operated with STM feedback, and simultaneous scans of STM topography, force and force gradient can be acquired.

The use of very small oscillation amplitudes at

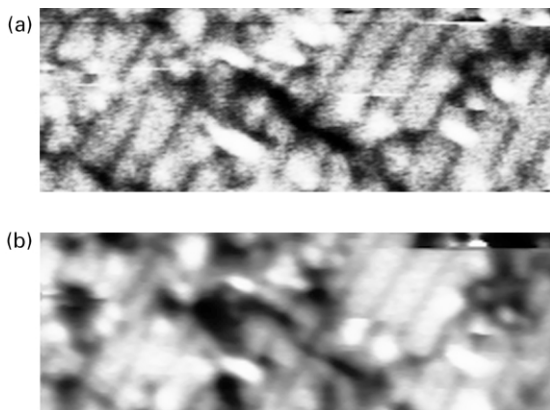


Fig. 2. Simultaneous STM (a) and force gradient (b) images of Si(100)(2 × 1). Image size is $110 \times 38 \text{ \AA}^2$, $V_{\text{tip}} = -1.5 \text{ V}$, $I_t = 0.5 \text{ nA}$, $A_0 = 2.4 \text{ \AA}$ and $k_0 = 157 \text{ N/m}$. Black areas correspond to more negative values in the force gradient image.

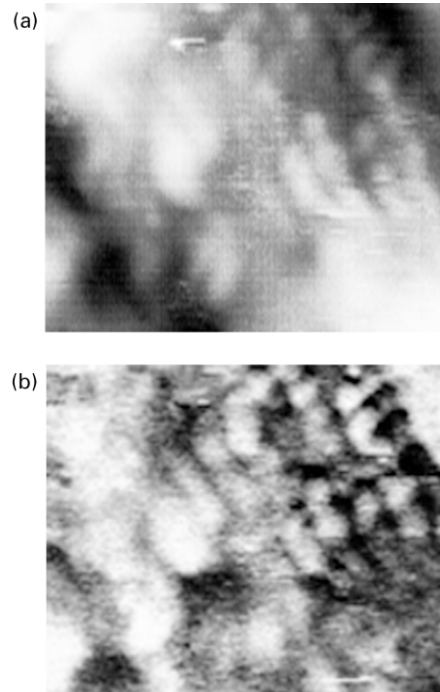


Fig. 3. Simultaneous STM (a) and force gradient (b) images of Si(100)(2 × 1). Image size is $55 \times 44 \text{ \AA}^2$, $V_{\text{tip}} = 1.5 \text{ V}$, $I_t = 0.5 \text{ nA}$, $A_0 = 0.5 \text{ \AA}$ and $k_0 = 70 \text{ N/m}$. Black areas correspond to more negative values in the force gradient image.

frequencies far below resonance allowed us to deduce the force gradient between tip and sample using a simple approximation:

$$dF/dz = k_0(1 - A_0/A),$$

where k_0 , A_0 and A are stiffness, free oscillation amplitude and the measured amplitude of the cantilever, respectively.

3. Results and discussions

In the first set of experiments, a lever with a resonance frequency of 23.2 kHz and a stiffness of about 157 N/m was used. Fig. 1 shows simultaneous force gradient and STM images of $154 \times 77 \text{ \AA}^2$ area of 2 × 1 reconstructed Si(100) surface. We unintentionally used a relatively large free oscillation amplitude of 2.4 Å at a frequency of 7.9 kHz in this run. Tip bias voltage and tunnel current were -1.5 V and 1 nA, respectively. Both of the images clearly show the dimer rows on the Si(100) surface. Some large area defects, such as missing dimer groups, are also visible in the images. In the force gradient images darker regions correspond to higher attractive force gradients. The dimer corrugation in the force gradient image is found to be about 3.4 N/m along the dimers. Another set of images of the same sample on a different area scanned with the same tip with a smaller tunnel current of 0.5 nA is shown in Fig. 2. The dimer rows,

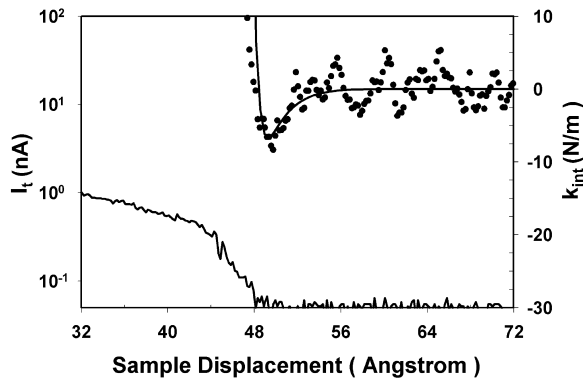


Fig. 4. Measured interaction stiffness (dotted line) and fit according to Rose potential (solid line), and tunnel current vs sample displacement. $A_0 = 0.25 \text{ \AA}$ and $k_0 = 110 \text{ N/m}$. $|E_b| = 3.25 \text{ eV}$, $\lambda = 1 \text{ \AA}$.

defects and contaminants are again visible in the force gradient and STM scans. The dimer corrugation in the force gradient image in Fig. 2 is about 2.3 N/m , which is lower than the corrugation in the previous scan (Fig. 1) taken with a tunnel current of 1 nA . There are some features which show up with a different contrast in STM and force gradient images in Figs. 1 and 2. This demonstrates that the STM and AFM contrast can be different. Since STM measures the local density of states around the Fermi level, an adsorbed atom on the surface resulting in a reduction of the density of states may be seen as a depression in the STM image, while it looks as a protrusion in the force image.

The dimer corrugation in another force gradient image taken with a tunnel current of 0.2 nA , which is not shown here, was found to be 1.98 N/m . If this information together with the dimer corrugations measured in force gradient images of Figs. 1 and 2 are considered, we end up with a monotonic relation between the dimer corrugation and the tip–sample separation during the scan. We observed a similar behavior for a $\text{Si}(111)(7 \times 7)$ surface [7].

Fig. 3 shows simultaneous force gradient and STM images of a different sample taken with a different tip, using an oscillation amplitude of 0.5 \AA . The stiffness of the lever is about 70 N/m . This time, not only the dimer rows, but also individual dimers on the surface next to an S_B type step at the upper right corner are also resolved in both images, with a relatively better contrast in the force gradient. In some of the scans, atomic resolution was achieved even in force images of the surface, which is measured from the deflection of the cantilever. The quality of the tip is the most important factor in our experiments.

We also carried out F–d spectroscopy experiments on a $\text{Si}(100)$ surface using W levers. In F–d measurements, force, force gradient, dissipation and tunnel current are recorded simultaneously as the sample is approached towards the tip and retracted back. The lever is dithered with typical oscillation amplitude of about 0.25 \AA . Since the oscillation amplitude is very small, the energy input to the

interacting tip–sample system is extremely low compared to the large amplitude measurements. Hence, the interaction is measured with a minimal external perturbation.

The F–d measurements revealed basically two groups of curves. Some of the tips give force gradient curves which exhibit a long interaction range which is an indication of long-range van der Waals and electrostatic forces dominating over short-range forces. In such measurements, the onset of tunnel current, which has a stronger separation dependence than force, is well after the point that a change in the force gradient starts. In contrast, some other tips allowed us to resolve the short-range force interactions between the tip and the sample. Fig. 4 shows such a force gradient curve along with the simultaneously acquired tunnel current as function of the displacement of the sample scan piezo. The dotted curve is the measured interaction stiffness (negative of the force gradient), whereas the solid line corresponds to a fit to the measured stiffness, the details of which are described below. The curves shown here are *single approach* curves and are not averaged over several measurements. The observable residual noise is due to the very low, 0.25 \AA , oscillation amplitude as well as the relatively short time constant used in the lock-in amplifier. Here, unlike the described long-range curves, the tunnel current rises at a position close to the onset of a remarkable change in the interaction stiffness. The tunnel current exhibits the expected exponential behavior. The interaction range in the force gradient curve is of the order of a few Ångströms, which is expected from an interacting system of an ideal tip and a clean surface. The maximum attractive force gradient is about 10 N/m . The whole approach and retraction process is reversible provided the separation is not reduced beyond the point at which the measured stiffness becomes positive.

We were only able to obtain atomic resolution in the force gradient images when the tip–surface interaction exhibited significant short-range contributions to the total force gradient. The tips that revealed a long overall length scale in force gradient curves did not allow us to resolve atoms in force gradient images. This confirms the theoretical expectation that short-range forces are required for atom resolved AFM [13], and is consistent with our previous work on a $\text{Si}(111)(7 \times 7)$ surface [7,12].

We compared our results with a simple model introduced by Rose et al. [14] which is shown to fit a wide range of atomic interactions with a suitable scaling of parameters. The tip–sample energy can be written as

$$E(z) = -|E_b|(1 + a + 0.05a^3)e^{-a},$$

where E_b is the minimum of the interaction potential, and a is the normalized distance given by

$$a = \frac{z - z_0}{\lambda}.$$

Here z_0 is a distance offset which results from the fact that the true zero of the distance axis is unknown, and λ is the

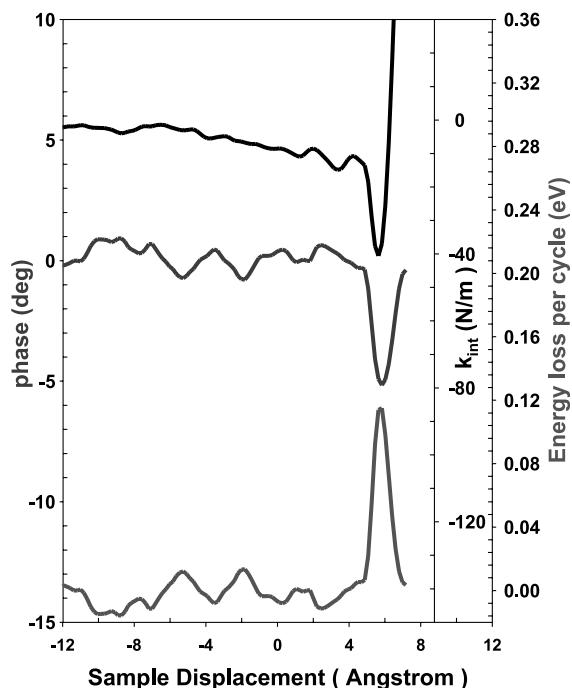


Fig. 5. Measured force gradient/phase/dissipation–distance curves on Si(100)(2 × 1), $A_0 = 0.25 \text{ \AA}$ and $k_0 = 130 \text{ N/m}$.

characteristic length scale (roughly the distance between the minimum of the interaction potential and its inflection point). We differentiated this universal energy curve twice to get k_{int} , and fitted the measured interaction stiffness in Fig. 4 to that expression. The fit shown by the solid line gives a value of 3.25 eV for E_b , and 1 Å for λ . These values are comparable with the values we have found for the interaction between a W tip and a Si(111)(7 × 7) surface [7, 12].

Fig. 5 shows a force gradient/phase/dissipation–distance curve obtained on another Si(100)(2 × 1) sample. The dissipation starts to increase as soon as the force gradient starts to decrease. It reaches a maximum value of 0.12 eV/cycle just after the minimum of the force gradient and starts to decrease unexpectedly as the sample is approached closer to the tip. This behavior is quite different from that found in large oscillation amplitude nc-AFM experiments [15], where only a gradual monotonic increase in the dissipation is observed as the sample is approached closer to the tip. We believe that our method gives more accurate results due to very small oscillation amplitudes we employ in our experiments.

4. Conclusion

In summary, we have imaged the Si(100)(2 × 1) surface

with nc-AFM/STM using sub-Ångstrom oscillation amplitudes for the first time. Quantitative atomic resolution force gradient images exhibiting individual dimers and atomic scale defects on the surface are obtained. F–d spectroscopy of the Si(100)(2 × 1) surface yields $\sim 3.3 \text{ eV}$ binding energy and short length scale for the interaction which is in reasonable agreement with the modeling. The measured dissipation in the tip reaches a maximum value of 0.12 eV/cycle and drops unexpectedly as the sample is brought closer to the tip. The tips which revealed force gradient curves with long interaction ranges did not give atomic resolution images, whereas atomic resolution force gradient images are obtained with the tips which are able to resolve short-range interatomic forces.

Acknowledgements

We are grateful to Professor Salim Çıracı for his continuous support and guidance as a teacher, mentor and friend over the years. This project is partially supported by The British Council and The NanoMagnetics Instruments Ltd [16].

References

- [1] G. Binnig, H. Rohrer, Ch. Gerber, E. Weibel, Appl. Phys. Lett. 40 (1982) 178.
- [2] S. Çıracı, in: R. Wiesendanger, H.-J. Güntherodt (Eds.), Scanning Tunneling Microscopy, vol. 3, Springer, Berlin, 1996, chapter 8.
- [3] G. Binnig, C.F. Quate, Ch. Gerber, Phys. Rev. Lett. 56 (1986) 930.
- [4] U. Dürig, O. Züger, D.W. Pohl, Phys. Rev. Lett. 65 (1990) 349.
- [5] G. Cross, A. Schirmeisen, A. Stalder, P. Grütter, M. Tschudy, U. Dürig, Phys. Rev. Lett. 80 (1998) 4685.
- [6] F.J. Giessibl, Science 267 (1995) 69.
- [7] A. Oral, R.A. Grimsble, H.Ö. Özer, P.M. Hoffmann, J.B. Pethica, Appl. Phys. Lett. 79 (2001) 1915.
- [8] R. Pérez, I. Stich, M.C. Payne, K. Terakura, Phys. Rev. B. 58 (1998) 10835.
- [9] A. Oral, R.A. Grimsble, H.Ö. Özer, J.B. Pethica, in preparation.
- [10] T. Uchihashi, Y. Sugawara, T. Tsukamoto, T. Minobe, S. Orisaka, T. Okada, S. Morita, Appl. Surf. Sci. 140 (1999) 304.
- [11] K. Yokoyama, T. Ochi, A. Yoshimoto, Y. Sugawara, S. Morita, Jpn. J. Appl. Phys. 39 (2000) L113.
- [12] P.M. Hoffmann, A. Oral, R.A. Grimsble, H.Ö. Özer, S. Jeffery, J.B. Pethica, Proc. R. Soc. Lond. A 457 (2001) 1161.
- [13] R. Pérez, M.C. Payne, I. Stich, K. Terakura, Appl. Surf. Sci. 123 (1998) 249.
- [14] J.H. Rose, J.R. Smith, F. Guinea, J. Ferrante, Phys. Rev. B 29 (1984) 2963.
- [15] T. Arai, M. Tomitori, Appl. Surf. Sci. 188 (2002) 292.
- [16] www.nanomagnetism-inst.com.